Understanding and correcting the spurious interactions in charged supercells

Samuel E. Taylor and Fabien Bruneval
CEA, DEN, Service de Recherches de Métallurgie Physique, F-91191 Gif-sur-Yvette, France
(Received 7 April 2011; published 15 August 2011)

The supercell technique is widely spread for the simulation of charged point defects. Charged defects in a supercell are unfortunately subjected to spurious image interactions, which are usually handled by introducing two correcting terms: a Madelung-type correction that accounts for the electrostatic interactions of repeated charges in a compensating background and a potential alignment term that refers the charged supercell to the electron reservoir. We demonstrate that the Madelung correction already brings a large potential shift that slowly converges as $1/L$ with increasing supercell sizes. We hence define a potential alignment devoid of any double counting. We finally propose a simple evaluation for the nearest-neighbor interaction that removes the remaining spurious hybridization of the defect wave functions between images. The application of these three corrections together drastically speeds up the convergence with respect to supercell size for all defects that are not too shallow.

DOI: 10.1103/PhysRevB.84.075155 PACS number(s): 71.15.Mb, 61.72.Bb

I. INTRODUCTION

The accurate prediction of the properties of point defects is a key target of computer simulations in condensed matter since defects govern many aspects of the physics of materials. For instance, applications in electronics, optoelectronics, and photovoltaics all rely on the fine control of charged defects in semiconductors.[1] With the advent of large supercomputers, it has been possible to address the *ab initio* calculation of point defects for over two decades now, thanks to density functional theory (DFT).[2]

The *ab initio* calculation of defects in condensed matter usually relies on the supercell approach.[3] In this framework, the *isolated* defect one intends to study is placed in a large cell, which is periodically replicated. The advantages of this approach are numerous, in particular the use of standard plane-wave codes. The supercell approach is so practical that it prevailed over competing frameworks, such as Mott-Littleton[4] or Korringa-Kohn-Rostoker Green's function.[5]

Nonetheless, the supercell approach suffers from one main drawback: the spurious interaction between the defect and its periodic images. This problem becomes particularly prominent for charged systems that are subjected to the long-range Coulomb interaction between images. No supercell size accessible to modern (or future) computers would be sufficient to render this interaction negligible. Indeed, the magnitude of this spurious contribution to the total energy scales as $N^{-1/3}$, with N being the number of atoms in the supercell.

This fact has given rise to the design of correction schemes that would accelerate the slow convergence of charged supercells. Correction schemes are numerous,[3,6–11] but they generally rely on the evaluation of two contributions: a correction of the energy and/or a correction of the potential. The correction for the energy ΔE_{el} is intended to remove the spurious long-ranged electrostatic interaction between the charged defect, its images, and the compensating background. The potential shift ΔV should account for the change of the reference energy for the electrons in the charged supercell compared to the electrons in the pristine bulk. Then the formation energy $E_f(D,q)$ of defect D with charge q in the Zhang and Northrup formalism[12] finally reads[13]

$$E_f(D,q) = E_{D,q} - E_{\text{Host}} - \sum_i n_i \mu_i + q(\epsilon_{\text{VBM}} + \epsilon_F + \Delta V) + \Delta E_{el}(q), \quad (1)$$

where $E_{D,q}$ is the raw energy of a supercell containing the defect D and an extra charge q and E_{Host} is the energy of the perfect supercell with no defect. The energy of the added or removed atoms n_i is referred to the chemical potential of reservoirs for the different elements μ_i. For electrons, the chemical potential is governed by the Fermi energy E_F, the zero of which is conventionally set at the valence band maximum of the bulk material ϵ_{VBM}.

Much effort has been devoted to the design of intelligent electrostatic corrections ΔE_{el}; comprehensive discussion on this point can be found elsewhere.[9,14–16] A multitude of conflicting ways have also been suggested to calculate the potential alignment, but no convincing arguments have yet been put forward for which is the most suitable. Some authors suggest taking an average of the total Kohn-Sham potential,[15,17,18] and others suggest an average of the electrostatic potential only.[13,19,20] This average is then taken either over the entire supercell[17,19] or in some localized region, usually as far as possible from the defect.[8,9,14] Some authors even refrain from including potential alignment at all, due to a (not entirely unfounded) fear of double counting some terms when employing an electrostatic correction and potential alignment together.[21] Even more worryingly, there seems to be a discontinuity in the community in the sign convention used when defining potential alignment. It appears that many authors take the potential shift defined in Eq. (1) as the average potential in the defect cell minus the average potential in the host cell, whatever their definition of these averages is,[20,22,23] while other authors do completely the opposite.[17,24]

Hence, the best way to proceed when attempting to improve the convergence for the supercell technique for charged defects is rather unclear. As a first illustrative example, we provide in Fig. 1 the convergence of the formation energy of two charged defects in silicon: the tetrahedrically coordinated

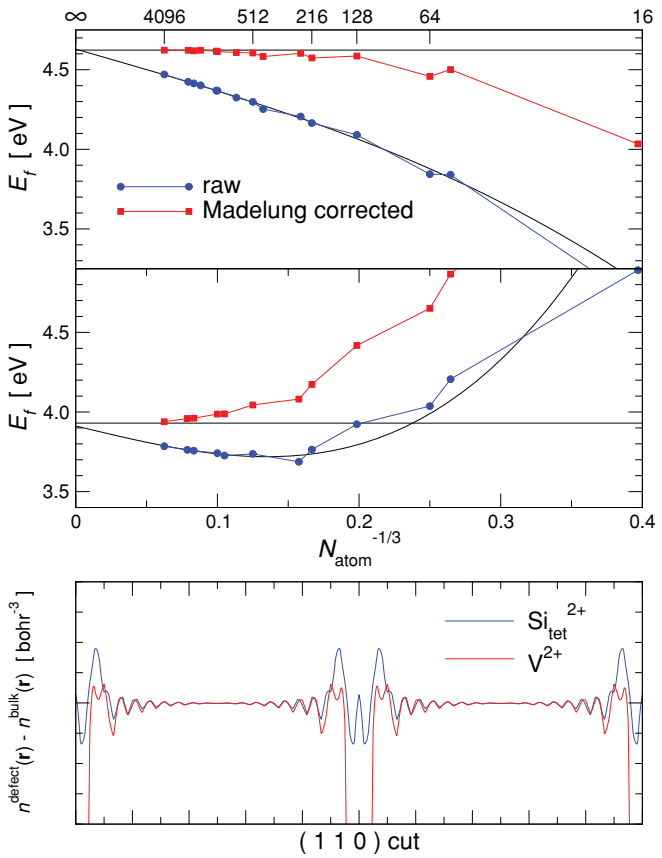

FIG. 1. (Color online) Convergence as a function of the supercell size of the formation energy (top) of a silicon interstitial Si_{Tet}^{2+} and (middle) of a silicon vacancy V_{Si}^{2+}. The raw energies are represented with circles. The Madelung corrected energies are represented with squares. The horizontal lines represent the converged values, and the thin dashed lines are tentative extrapolations with the usual function $\gamma_1 N^{-1/3} + \gamma_2 N^{-1}$. (bottom) A cut of the difference in electronic densities between the defective and host cells, $n^{\text{defect}}(\mathbf{r}) - n^{\text{bulk}}(\mathbf{r})$, along the (110) direction, passing through the bond centers for a 1000-atom cubic supercell.

self-interstitial Si_{Tet} (top panel) and the silicon vacancy V_{Si} (middle panel). The two defects have been considered in their 2+ charge state. For this charge state, they both have no occupied state in the band gap. They are both embedded in the same silicon host. In principle, one could have expected the same behavior as a function of the supercell size. Figure 1 obviously contradicts this prediction. The uncorrected data monotonously converge with a quite fair $N^{-1/3}$ behavior in the case of Si_{Tet}^{2+}. In the case of V_{Si}^{2+}, the convergence experiences a turning point. The inclusion of the simple Madelung electrostatic correction performs very well for the former and very poorly for the latter. This different behavior could not easily be anticipated from the electronic structure. The bottom panel of Fig. 1 shows a cut of the difference of electronic density between the defective and pristine supercells. Except in the vicinity of the defect, the electronic density differences at middle range simply show some Friedel's type oscillations with similar amplitudes. This clearly shows that the solution to the problem does not lie in an improved definition of electrostatic corrections.

In this article, we carefully address the different errors affecting the energy obtained in supercell calculations. We leave aside the elastic relaxations that produce much weaker effects, and we concentrate on the electronic structure problems. We summarize the computational aspects in Sec. II. In Sec. III, we demonstrate that the electrostatic interactions induce a position-dependent shift in the potential. As a consequence, the definition of the potential alignment should be revised to ensure the electrostatic contribution is not erroneously double counted. Furthermore, our proposed potential alignment is opposite in sign to some definitions (Sec. IV). We finally identify a prominent contribution to the error in the supercell technique: the spurious hybridization of defect wave functions onto several images. This contribution is usually completely disregarded. We provide in Sec. V a simple and practical way to evaluate this involved term. The performance of our three corrections is then demonstrated using various typical examples.

II. COMPUTATIONAL DETAILS

All the DFT calculations presented here utilized the local density approximation (LDA) for the exchange-correlation functional, as implemented within the plane-wave code ABINIT.[25] Norm-conserving Troulliers-Martins[26] pseudopotentials were used for sodium and chloride, with only the 1*s* electrons treated as core for sodium. For silicon, we developed an extremely smooth pseudopotential using the FHI-98PP program.[27] This pseudopotential has a very large cutoff radius of 4.0 bohr for both the *s* and the *p* channels. This somewhat crude pseudopotential yields a surprisingly good lattice parameter (5.408 Å) and defect formation energies. The very low plane-wave cutoff of 2.0 Ha enabled us to study phenomenally large supercells (up to 4096 atoms). For NaCl and for Si, $4 \times 4 \times 4$ and $2 \times 2 \times 2$ shifted Monkhorst-Pack[28] *k*-point grids were used for primitive cells and supercells, respectively. A lattice constant of 5.646 Å was used for NaCl, and the cells were left unrelaxed throughout the calculations. For silicon, following Ref. 9, the four neighbors nearest to the defect have been relaxed in the 64-atom cell, and these positions of the nearest neighbors are used for all further calculations.

III. EVALUATING THE POTENTIAL SHIFT INDUCED BY THE ELECTROSTATIC CORRECTION

In this section, we demonstrate that the electrostatic correction ΔE_{el} and the potential alignment ΔV are, indeed, connected quantities. Having this connection in mind will allow us to propose an evaluation of the potential alignment that does not double count the spurious electrostatic potential of the supercell approach.

In order to keep the discussion simple we consider here the simplest electrostatic correction, the monopole Madelung term, as first proposed by Leslie and Gillan:[3]

$$\Delta E_{el} = E_{el}^{\text{isolated}} - E_{el}^{\text{periodic}} \approx \frac{\alpha q^2}{2\epsilon L}, \qquad (2)$$

where α is the Madelung constant of the lattice, q is the unbalanced charge, and L is the edge of the periodic box. The

monopole correction is designed to transform the electrostatic energy of a lattice of point charges in a neutralizing background into the electrostatic energy of a single point charge. In polarizable medium such as a solid, the Coulomb interaction is further screened by the electrons, and the electrostatic energy should be divided by the electronic dielectric constant ϵ. Here we use ϵ_∞ since the atoms are not allowed to relax in the present study.

Some authors attempt to improve convergence by including the third-order quadrupole in the electrostatic correction. We have avoided doing this for three reasons. First, one of our primary aims in this work was to produce an effective, useful, and, crucially, *simple* correction scheme. Hence, we utilize the simplest possible electrostatic correction. Second, as mentioned in Sec. I, the similarity in the electronic density difference between two silicon defects that converge at vastly different rates proves that improving our definition of the electrostatic correction will not solve the problem. In fact, this electronic density difference is the key quantity in the quadrupole term, lending further weight to this assumption. Finally, a relatively recent study[8] showed that the quadrupole correction does not always improve results, leaving its utility somewhat in question. In fact, since the quadrupole term always acts in the opposite direction to the Madelung monopole, it will always worsen results for defects that are converging from below after the monopole correction has been applied (e.g., the silicon interstitial in Fig. 1).

Let us now prove rigorously that the monopole term in Eq. (2) already introduces a shift in the potentials. The Kohn-Sham (KS) potential $v_{\rm KS}$ is obtained by the functional derivative of the total energy minus the kinetic energy with respect to the electronic density $n(\mathbf{r})$:[2]

$$v_{\rm KS}(\mathbf{r}) = \frac{\delta(E[n] - T[n])}{\delta n(\mathbf{r})}. \tag{3}$$

If the energy $E[n]$ requires an electrostatic correction ΔE_{el}, so will the obtained potential.

The functional derivative of the KS potential with the electrostatic correction can easily be tracted if the expression of the charge q as a function of the density is introduced:

$$q = \sum_i Z_i - \int d\mathbf{r} n(\mathbf{r}), \tag{4}$$

where $\sum_i Z_i$ is the total of the ionic charges in the cell.

Hence, the periodic KS potential also contains a spurious contribution when compared to the isolated KS potential, if one assumes a monopole correction:

$$v_{\rm KS}^{\rm periodic}(\mathbf{r}) = v_{\rm KS}^{\rm isolated}(\mathbf{r}) - \frac{d}{dq}(-\Delta E_{el}) \tag{5}$$

$$= v_{\rm KS}^{\rm isolated}(\mathbf{r}) + \frac{\alpha q}{\epsilon_\infty L}, \tag{6}$$

where the minus sign in the first line comes from the differentiation of Eq. (4) with respect to the electronic density. Finally, we see the KS potential in a periodic supercell is shifted with respect to the KS potential that an isolated charge would have, by the Madelung potential constant v_M, which reads[11]

$$v_M = -\frac{\alpha q}{\epsilon_\infty L}. \tag{7}$$

We have thus demonstrated that the charged-supercell approach introduces a significant shift in the KS potentials, which slowly decays as $1/L$. Therefore, one cannot consider independently correcting the electrostatic energy and correcting via potential alignment.

Keeping this in mind, what should be the practical procedure to perform a consistent, reliable potential alignment? In order to approach this problem, we have implemented a simple Poisson solver for periodic systems, based on fast Fourier transforms, completely analogous to the technique used in periodic DFT codes. This code allowed us to produce the data for Fig. 2 that present the electrostatic potential of a positive point charge (in reality, a Gaussian with a very small width) as it would be calculated in any periodic code. The parameters were chosen to represent a positive charge, located at zero in a cubic 512-atom supercell of sodium chloride. The interactions were scaled down with the calculated dielectric constant ϵ_∞. The choice of NaCl is governed by the desire to have localized defects that ease understanding.

A truly isolated point charge q in a medium should create a long-range Coulomb potential $q/\epsilon_\infty r$, as represented by a solid line in Fig. 2. The potential created by the truly isolated point charge goes asymptotically to zero. The calculated electrostatic potential of a point charge in a supercell with a compensating background, represented by the dashed line, deviates significantly from the single isolated charge. In

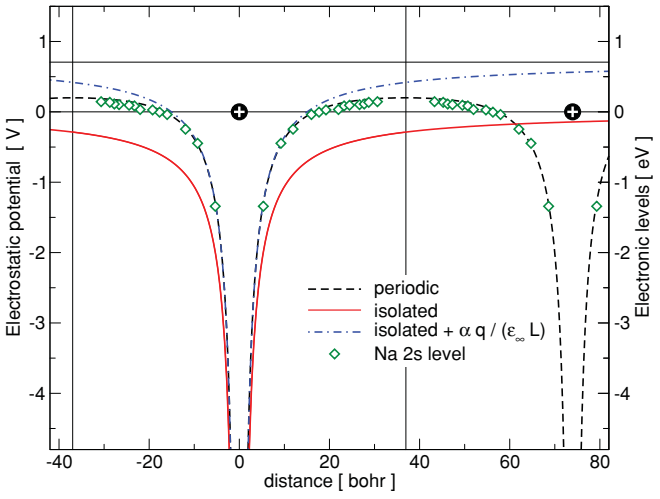

FIG. 2. (Color online) Electrostatic potentials created by a single point charge in an infinite sample (solid red line), an array of point charges with compensating background (dashed black line), and a single point charge in an infinite sample shifted by the Madelung potential $-v_M$ (dot-dashed blue line). The parameters (lattice constant, dielectric constant) have been chosen to mimic a cubic 512-atom supercell of NaCl. The green diamonds represent the deviation of the Na 2*s* core levels with respect to the bulk Na 2*s* levels, as obtained from a real calculation of a 512-atom supercell containing a vacancy $V_{\rm Cl}^+$. The horizontal lines show the asymptotic values of the single point charge potentials.

the vicinity of the charge, the periodic potential appears as shifted with respect to the isolated potential. At the box boundary, the periodic potential experiences the two neighboring point charges equally and therefore shows a spurious plateau shape. We also introduced, with a dot-dashed line, the isolated potential shifted by the Madelung potential v_M following Eq. (5). We observe that this shifted potential closely reproduces the periodic potential in the vicinity of the point charge but asymptotically converges to $-v_M$. The divergence of the shifted isolated point-charge potential from the KS potential further away from the point charge would be reduced if higher-order terms in the Makov-Payne expansion were considered in Eq. (2). It is now obvious that the difference between the periodic potential and the shifted isolated potential is worst at the box boundary. Finally, in order to demonstrate that our modeling bears some connection to reality, we added the deviation in the $2s$ level of sodium with respect to bulk in an actual 512-atom supercell calculation of a chlorine vacancy V_{Cl}^{+}. As shown by the diamonds in Fig. 2, the calculated points and the periodic potential agree impressively well. The positions of the Na$2s$ levels are simply governed by the screened electrostatic potential of the periodically replicated charges in a compensating background.

Many authors have prescribed performing the potential alignment by considering the electrostatic potential far from the charged defect as the zero of the potential.[8,9,13] In our opinion, this approach presents several problems. First of all, applying an electrostatic energy correction already brings about a shift in the potential, proportional to $1/L$. There is no need, therefore, to introduce another electrostatic potential alignment term that also goes as $1/L$, as this leads to double counting the same contribution. Second, when considering an energy correction brought about by an electrostatic potential shift, one needs to divide by a factor of 2, as shown when going from Eq. (7) to Eq. (2). This is not always clear in other potential alignment methods. Third, no matter how far from the defect one measures the potential alignment and no matter how large one makes the supercell, one can never recover the infinite-limit correct potential, with its long-range $1/r$ behavior. Fourth, considering the potential far from the defect is precisely the position where the deviation of the periodic potential from the isolated charge is the most striking: at the box boundary, the potential is equally generated by charges from different cells.

These conclusions show the crucial need to redefine the potential alignment. This is the topic of the next section.

IV. DEFINING THE PROPER POTENTIAL ALIGNMENT

Our goal is now to find a proper definition for the potential alignment ΔV introduced in Eq. (1). Potential alignment is needed for charged defects since the formation energy of a charged defect is a function of the Fermi level ϵ_F, i.e., the energy of the electrons from a reservoir. The energy zero is conventionally set to the top valence band of the bulk material, and the Fermi level is usually varied within the range of the band gap.

It was recognized very early on that the band structures of defective supercells are shifted with respect to their pristine counterparts and that, therefore, a potential alignment correction was needed.[29] Unfortunately, the potential alignment correction was mainly thought to correct for the spurious electrostatic potential, even though this contribution is usually already corrected through the electrostatic correction. Our definition for the potential alignment is, therefore, deliberately set up to ensure the electrostatic correction is not double counted. We suggest a correction that provides a naïve, extremely simple measurement of the potential shift yet performs surprisingly well, as we will show in the following.

We propose a scheme similar to that suggested in Ref. 17, whereby the average of the *total* potential over the *entire* supercell $\langle v_{KS} \rangle$ is considered:

$$\langle v_{KS} \rangle = \frac{1}{\Omega} \int_{\Omega} d\mathbf{r} v_{KS}(\mathbf{r}), \tag{8}$$

where Ω is the volume of the supercell. Why do we focus on this particular quantity?

First, the total average potential is completely free of any electrostatic contribution. Indeed, the average value of the electrostatic potential in a periodic cell is conventionally set to zero; otherwise, it would give rise to divergent terms. By considering the average potential we ensure that the electrostatic potential shift does not enter into the correction again, having already taken care of it via the previously defined ΔE_{el} term.

Second, a reference electron from the reservoir is one delocalized in a region infinitely far from the defect. In Fig. 3, this ideal situation is represented in the top schematic. The delocalized electron experiences the KS potential of the perfect bulk averaged over a large region. In practice, however, we perform a supercell calculation (schematic in the bottom panel of Fig. 3) where there is no region of space unaffected by the defect. An infinitely distant delocalized electron would

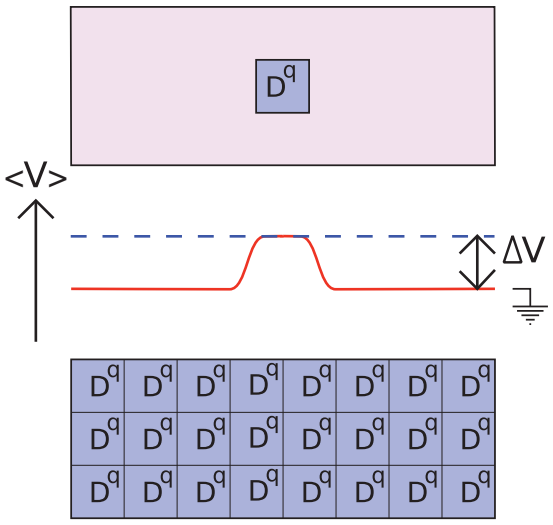

FIG. 3. (Color online) Schematics illustrating the role of the potential alignment ΔV. (top) The system we intend to simulate: a single charged defect D^q in a single supercell (dark blue), embedded in the infinite bulk (light pink). (bottom) The system we actually calculate with the supercell approach: an array of replicated defects D^q. (middle) The corresponding running average potentials, with a solid red line for the truly isolated defect and a dashed blue line for the supercell approach.

experience the KS potential of the defective supercell averaged over a large region. The potential alignment ΔV represented in the middle panel should, therefore, bring the average potential of the defective cell onto the reference average potential of the bulk cell:

$$\Delta V = \langle v_{\mathrm{KS}}^{\mathrm{bulk}} \rangle - \langle v_{\mathrm{KS}}^{\mathrm{defect}} \rangle. \tag{9}$$

Note that this definition of the potential alignment differs in sign with respect to the definition of some authors.[9,23] This potential alignment clearly states that the average potential obtained from supercell calculations is erroneous and should be corrected to fit the average potential of the pristine bulk. Finally, it should also be noted that the value defined in Eq. (8) is part of the standard output of the electronic structure code used in this study,[25] making evaluation of the potential alignment defined in Eq. (9) extremely quick and simple.

Let us demonstrate for a selected case the quality of the potential alignment we proposed in Eq. (9). As we intend to isolate the effect of potential alignment without the other corrections, we need it to be sizable. In Fig. 4 we considered the negatively charged sodium vacancy in NaCl. This particular case was chosen because one could expect a good performance of the Madelung correction in this defect. Indeed, the charge associated with the defect is very well localized; it is almost a point charge even for the smallest supercells. An informative sample case is a defect that is well converged after applying an electrostatic correction and potential alignment. We need this to hold even for small supercells, for which the potential alignment is large and its effect can be seen most clearly. The highly localized, nonshallow nature of the sodium vacancy allows it to agree with this demonstrative requirement.

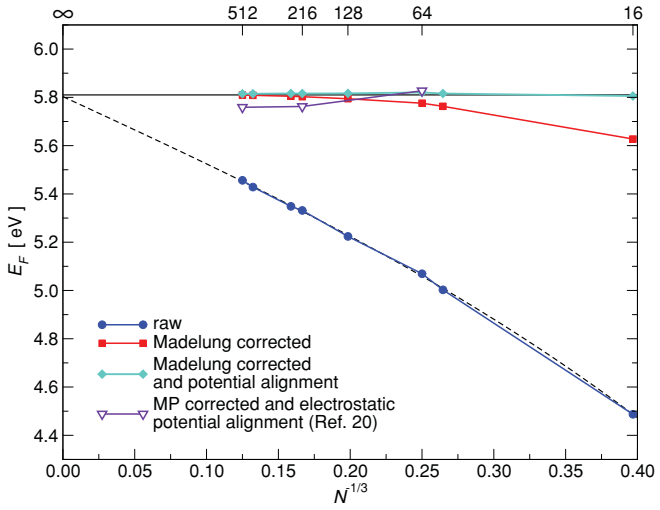

FIG. 4. (Color online) Convergence as a function of the supercell size of the formation energy of a sodium vacancy V_{Na}^{-}. The raw energies are represented with circles. The Madelung corrected energies are represented with squares. The data with potential alignment following Eq. (9) together with the Madelung correction are represented by diamonds. The data with potential alignment following Ref. 9 together with the Makov-Payne monopole and quadrupole corrections are represented by open triangles. The horizontal line represents our converged value, and the thin dashed line is a tentative extrapolation with the usual function $\gamma_1 N^{-1/3} + \gamma_2 N^{-1}$.

After the usual Madelung correction, the potential aligned data in Fig. 4 using Eq. (9) converge to the asymptotic value extremely quickly. Note that with a supercell as small as 16 atoms, the potential alignment $q\Delta V$ is as large as 0.18 eV, and applying it (along with the Madelung correction) leads to a corrected formation energy less than 10 meV from its converged value. This is somewhat compelling evidence that the sign convention we introduced in Eq. (9) is correct. For comparison, we also show in Fig. 4 results obtained with a quite popular alternative correction scheme, which combines the Makov-Payne correction (including terms up to the quadrupole) and an electrostatic potential alignment, as detailed in Ref. 9. As shown clearly in Fig. 4, our scheme appears to be converging to a slightly different value and at a much faster rate. Another correction scheme, detailed in Ref. 10, has already been shown to yield similar results to ours in the case of defects in NaCl, although it is rather more complicated to implement.

Note also that the potential alignment goes to zero very fast for larger supercells, as predicted. This may explain why, to date, it has proved difficult for the defect community to reach an agreement on the definition of potential alignment.

V. CORRECTING THE REMAINING NEIGHBOR'S INTERACTION

After correcting the electrostatic energy and the Fermi level with potential alignment, we are still left with some unexplained, slowly converging terms. For instance, neutral defects, which are unaffected by the two aforementioned corrections, may sometimes also experience a very slow convergence.[30,31] This behavior can be attributed, at least in part, to the quantum interaction between the defect and its images. Instead of being localized around one single defect, the defect-related wave functions can be delocalized over several images. This hybridization may lead to a change in the defect energy.

A similar behavior is observed and well documented in the context of adatoms on surfaces, where effective lattice gas models have been introduced.[32] We will now follow the same philosophy but simplify the situation by considering only a single kind of neighbors. The effective Hamiltonian H_n for a defect in a supercell interacting with n neighbors of the same kind reads

$$H_n = H_0 + nV, \tag{10}$$

where H_0 is the effective Hamiltonian with no neighbor interactions and V is the magnitude of the neighbor-neighbor interaction. The Hamiltonian H_0 is the target quantity, and H_n is the quantity obtained from a supercell calculation. In the modeling of Eq. (10) we assumed two-body interactions only.

We then propose to fit the two parameters H_0 and V of the model in Eq. (10) with two *ab initio* calculations. The first calculation is of a regular supercell, and the second calculation uses a nonregular supercell, for which one direction has been doubled. In doing so and assuming the next-nearest-neighbor interactions are small, we vary the number of interacting neighbors n and hence can extract the two parameters of the model.

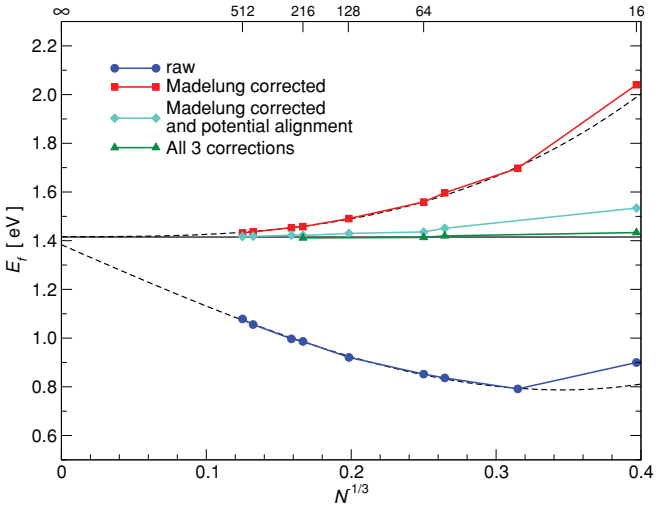

FIG. 5. (Color online) Convergence as a function of the supercell size of the formation energy of a chlorine vacancy V_{Cl}^{+}. The raw energies are represented with circles. The Madelung corrected energies are represented with squares. The data with potential alignment following Eq. (9) together with the Madelung correction are diamonds. The triangles represent the final data including the removal of the neighbor interaction according to Eq. (10). The horizontal line represents the converged value, and the thin dashed lines are tentative extrapolations with the usual function $\gamma_1 N^{-1/3} + \gamma_2 N^{-1}$.

The method is better explained with a practical example. We consider the chlorine vacancy V_{Cl}^{+} in NaCl in Fig. 5. In this case, again, the Madelung correction together with the potential alignment already yields a significantly improved result: the 16-atom supercell is converged to within 0.12 eV. NaCl is a textbook example for an ionic compound. The binding of the crystal is mediated through the isotropic Coulomb interaction. It is hence most probable that the defect states are isotropic too. As a consequence, we will assume that doubling the supercell in one direction will cut the magnitude of the interaction with neighbors by half. In practice, a calculation for a 16-atom face-centered-cubic supercell ($2 \times 2 \times 2$ unit cells) provided the value for $H_n = 1.50$ eV (after applying the Madelung correction and potential alignment), and a calculation for a 32-atom elongated face-centered-cubic supercell ($4 \times 2 \times 2$ unit cells) set the value for $H_{n/2} = 1.45$ eV. The extrapolated value for no defect-defect interactions is then easily obtained: $H_0 = 1.40$ eV, which lies within 0.02 eV of the converged value. The same procedure was also performed for larger supercells with a very good accuracy, as shown in Fig. 5. Our approach appears to be computationally relevant as well since the calculations of two small supercells (16 atoms and 32 atoms) offer an accuracy superior to the calculation with 64 atoms.

The model we propose considerably speeds up the convergence with respect to supercell size, at the expense of two calculations instead of one and some knowledge of the system under study. The approach crucially relies on the identification of the important directions of the crystal, with respect to the defect-defect interactions. In the case of NaCl, we assumed that all directions are equally important. However, returning to the case of silicon that we used as an introduction, we assume that the defect-defect interactions are preferentially mediated along the (110) zigzag chains of the diamond structure.[20] We thus considered the neighbors in these directions as the most relevant for the hybridization of defect states and set the values of n in Eq. (10) accordingly. When using a face-centered-cubic supercell, the (110) directions are, indeed, the first-nearest neighbors, and moving from a regular supercell to one doubled in one direction drops the number of nearest neighbors from 12 to 6.

When using a simple cubic supercell, it is the *second*-nearest neighbors that lie in the (110) directions. For extremely small simple cubic supercells, the assumption that the hybridization occurs only along the (110) directions is doubtful since the (100) neighbors are much closer. However, in order to assess the simplicity and the robustness of the present scheme, we will stick to our convention. For cubic supercells, the number of (110) neighbors drops from 12 to 4 when the length of one side of the cell is doubled. We used this framework to produce Fig. 6. First, note once again the performance of our potential alignment represented

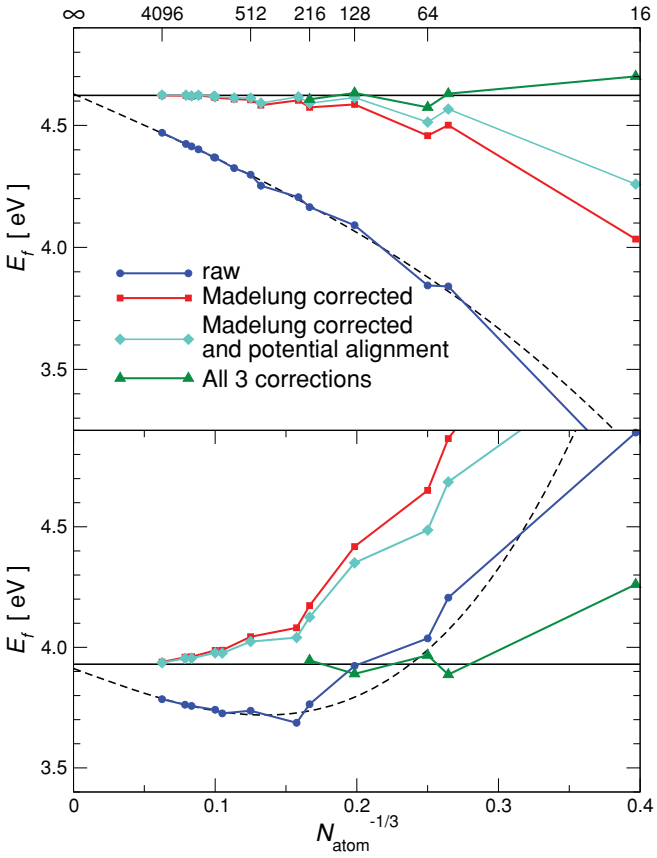

FIG. 6. (Color online) Convergence as a function of the supercell size of the formation energy of (top) a silicon interstitial Si_{Tet}^{2+} and (bottom) a silicon vacancy V_{Si}^{2+}. The raw energies are represented with circles. The Madelung corrected energies are represented with squares. The data with potential alignment following Eq. (9) together with the Madelung correction are diamonds. The triangles represent the final data, which include the removal of the neighbor interaction according to Eq. (10). The horizontal lines represent the converged value, and the thin dashed lines are tentative extrapolations with the usual function $\gamma_1 N^{-1/3} + \gamma_2 N^{-1}$.

with the diamonds. The triangles then show the final result of the present study including our three corrections. The agreement with the converged value is impressively good even for supercells as small as 54 atoms. The effect of the shape of the supercells becomes obvious: all the face-centered-cubic supercells converge to the asymptotic value from one side, and all the simple cubic supercells converge from the other. Finally, we should stress that this hybridization correction can also be utilized in the case of troublesome neutral defects. Indeed, the correction should prove particularly useful in these cases since the electrostatic and potential alignment terms do not apply.

VI. CONCLUSIONS

Calculations of charged point defects within the supercell approach are impossible to converge with a brute-force approach. Even our calculated 4096-atom supercells for defects in silicon still deviate largely from the asymptotic values. This makes it clear that more subtle approaches need to be designed and implemented. Many previous works addressed this issue, utilizing many different approaches, but the situation remains rather unsatisfactory.

The present contribution is twofold: a theoretical derivation that demonstrates that the spurious electrostatic energy introduced by the nonbalanced charge in the supercell induces a shift in the potential and a practical scheme using three simple corrections that significantly improve the convergence of the supercell approach.

The practical scheme we propose is extremely robust and simple and does not require additional coding. The only unconventional data needed here are the Madelung constant for nonregular cells. Our scheme reads (i) electrostatic correction, (ii) potential alignment, and (iii) hybridization correction. We showed that the simplest electrostatic correction of all, namely, the Leslie-Gillan Madelung correction,[3] is sufficient. We then showed that, if this electrostatic correction is applied, the potential alignment should be based on the *total average* Kohn-Sham potential to avoid double counting of the slowly converging $1/L$ term. Note that our definition uses a sign convention opposite to the definition of many authors. Finally, we could reduce the error due to the hybridization of defect states onto several images by using a simplistic model Hamiltonian and fitting it with two *ab initio* calculations. This hybridization correction could also be applied just as well, in principle, to the case of a slowly converging neutral defect.

Even though all the calculations presented here were based on local density approximation (LDA), the scheme could also be used in combination with hybrid functionals or the GW approximation.[33–35] The only cases that cannot be corrected within our scheme are those of shallow defect states, which are delocalized over regions that are impossible to fit into a tractable supercell. Besides this limitation, the efficiency and accuracy of our scheme has been impressive for all the cases tested so far.

ACKNOWLEDGMENTS

We acknowledge exciting discussions with J.-P. Crocombette and G. Roma and thank M.-C. Marinica for pointing out to us the literature on lattice gas models. This work was performed using HPC resources from GENCI-CINES and GENCI-CCRT (Grant No. 2011-gen6018).

[1] G. Grosso and G. Pastori Paravicini, *Solid State Physics* (Academic, San Diego, 2000).
[2] R. G. Parr and W. Yang, *Density-Functional Theory of Atoms and Molecules* (Oxford University Press, New York, 1989).
[3] M. Leslie and M. J. Gillan, J. Phys. C **18**, 973 (1985).
[4] A. B. Lidiard, J. Chem. Soc. Faraday Trans. 2 **85**, 341 (1989).
[5] A. R. Williams, J. F. Janak, and V. L. Moruzzi, Phys. Rev. B **6**, 4509 (1972).
[6] G. Makov and M. C. Payne, Phys. Rev. B **51**, 4014 (1995).
[7] P. A. Schultz, Phys. Rev. Lett. **84**, 1942 (2000).
[8] C. W. M. Castleton, A. Höglund, and S. Mirbt, Phys. Rev. B **73**, 035215 (2006).
[9] S. Lany and A. Zunger, Phys. Rev. B **78**, 235104 (2008).
[10] C. Freysoldt, J. Neugebauer, and C. G. Van de Walle, Phys. Rev. Lett. **102**, 016402 (2009).
[11] N. D. M. Hine, K. Frensch, W. M. C. Foulkes, and M. W. Finnis, Phys. Rev. B **79**, 024112 (2009).
[12] S. B. Zhang and J. E. Northrup, Phys. Rev. Lett. **67**, 2339 (1991).
[13] C. G. van de Walle and J. Neugebauer, J. Appl. Phys. **95**, 3851 (2004).
[14] A. Janotti and C. G. Van de Walle, Phys. Rev. B **76**, 165202 (2007).
[15] S. B. Zhang, J. Phys. Condens. Matter **14**, R881 (2002).
[16] P. Erhart, K. Albe, and A. Klein, Phys. Rev. B **73**, 205203 (2006).
[17] J. Shim, E.-K. Lee, Y. J. Lee, and R. M. Nieminen, Phys. Rev. B **71**, 035206 (2005).
[18] T. Mattila and A. Zunger, Phys. Rev. B **58**, 1367 (1998).
[19] D. B. Laks, C. G. Van de Walle, G. F. Neumark, P. E. Blöchl, and S. T. Pantelides, Phys. Rev. B **45**, 10965 (1992).
[20] S. Lany and A. Zunger, Modell. Simul. Mater. Sci. Eng. **17**, 084002 (2009).
[21] W. Chen, C. Tegenkamp, H. Pfnur, and T. Bredow, Phys. Rev. B **82**, 104106 (2010).
[22] C. Persson, Y.-J. Zhao, S. Lany, and A. Zunger, Phys. Rev. B **72**, 035211 (2005).
[23] S. Pöykkö, M. J. Puska, and R. M. Nieminen, Phys. Rev. B **53**, 3813 (1996).
[24] Y. Cui and F. Bruneval, Appl. Phys. Lett. **97**, 042108 (2010).
[25] X. Gonze, B. Amadon, P. M. Anglade, J. M. Beuken, F. Bottin, P. Boulanger, F. Bruneval, D. Caliste, R. Caracas, M. Cote, T. Deutsch, L. Genovese, P. Ghosez, M. Giantomassi, S. Goedecker, D. R. Hamann, P. Hermet, F. Jollet, G. Jomard, S. Leroux, M. Mancini, S. Mazevet, M. J. T. Oliveira, G. Onida, Y. Pouillon, T. Rangel, G. M. Rignanese, D. Sangalli, R. Shaltaf, M. Torrent, M. J. Verstraete, G. Zerah, and J. W. Zwanziger, Comput. Phys. Commun. **180**, 2582 (2009).
[26] N. Troullier and J. L. Martins, Phys. Rev. B **43**, 1993 (1991).

[27]M. Fuchs and M. Scheffler, Comput. Phys. Commun. **119**, 67 (1999).
[28]H. J. Monkhorst and J. D. Pack, Phys. Rev. B **13**, 5188 (1976).
[29]A. Garcia and J. E. Northrup, Phys. Rev. Lett. **74**, 1131 (1995).
[30]M. I. J. Probert and M. C. Payne, Phys. Rev. B **67**, 075204 (2003).
[31]A. F. Wright, Phys. Rev. B **74**, 165116 (2006).
[32]C. Stampfl, H. J. Kreuzer, S. H. Payne, H. Pfnür, and M. Scheffler, Phys. Rev. Lett. **83**, 2993 (1999).
[33]F. Oba, A. Togo, I. Tanaka, J. Paier, and G. Kresse, Phys. Rev. B **77**, 245202 (2008).
[34]F. Bruneval, Phys. Rev. Lett. **103**, 176403 (2009).
[35]M. Giantomassi, M. Stankovski, R. S. M. Grüning, F. Bruneval, P. Rinke, and G.-M. Rignanese, Phys. Status Solidi B **248**, 275 (2011).